scientific reports

Check for updates

OPEN

Potassium permanganate dye removal from synthetic wastewater using a novel, low-cost adsorbent, modified from the powder of *Foeniculum vulgare* seeds

Suhair. A. Bani-Atta

In this study, Seeds powder of *Foeniculum vulgare* was used to prepare a novel adsorbent, the modification of the prepared adsorbent was done by each of $ZnCl_2$, oxalic acid, and CuS, all samples have been characterized by different techniques and examined for Potassium permanganate ($KMnO_4$) adsorption. Among the four modified and unmodified adsorbents, the sample modified by oxalic acid has the highest percentage removal for $KMnO_4$ adsorption (%R = 89.36). The impact of $KMnO_4$ concentration, adsorbent dose, contact temperature, contact time, and solution pH on the adsorption performance was also investigated. The experimental data of this adsorption was analyzed by different kinetic and isotherm models. As Constants of thermodynamic ΔG°, ΔH°, and ΔS° have been also evaluated. Surface area, pore volume, and pore size of the modified oxalic acid *F. vulgare* seeds powder adsorbent were determined as 0.6806 $m^2\ g^{-1}$, 0.00215 $cm^3\ g^{-1}$, and 522.063 Å, as pH_{ZPC} also was stated to be 7.2. The R^2 values obtained from applying different isotherm and kinetic models (0.999 and 0.996) showed that the adsorption performance of $KMnO_4$ follows the Langmuir and Pseudo 2nd order models. Furthermore, high adsorption capacities of 1111.11, 1250.00, and 1428.57 mg g^{-1} were achieved at three temperatures that were used in this study. Constants of thermodynamic ΔG°, ΔH°, and ΔS° values indicate chemical and spontaneous adsorption at the adsorbent surface. Therefore, the modified adsorbent can be used to remove $KMnO_4$ dye from pollutant water samples.

Potassium permanganate ($KMnO_4$) is a highly strong oxidizing agent that is commonly used for water purification from numerous pollutants, mainly for the destruction of compounds that cause undesirable taste, odor, and color for the treated water[1]. Remarkably, permanganate is still one of the most oxidizing chemicals ever applied to remove each iron, manganese, and arsenic from water[2,3], In addition to its great ability to oxidize cyanide, phenols, and organic compounds[4–8].

Recently, many studies reported that excessive exposure to $KMnO_4$ may cause acute problems of the nervous system, irritation of the skin and eye, Furthermore, it was stated that manganese has significant toxicity towards the liver and kidneys[9,10]. Therefore many techniques and methods have been applied for $KMnO_4$ removal from the contaminated water. For instance, fluidized-bed crystallization method was used[11], concerning the ease of preparation and use, in addition to the high capacity to get rid of permanganate from wastewater adsorption is one of the most extensively utilized processes with different adsorbents[1], activated carbon is a common adsorbent that used for adsorption of $KMnO_4$ from polluted water due to its high adsorption efficiency[12,13].

To remove $KMnO_4$ molecules from polluted aqueous solutions by adsorption a lot of activated carbon adsorbents were prepared using shells of coconut[12], corn cob, and animal bone were also applied[14], sulfuric acid modification of activated carbon, and activated charcoal have been used too[1,15]. More recently, Nanoparticles of metallic oxides have been used to remediate effluent from various dyes[16–22], Copper sulfide nanoparticles were used as dynamic adsorbents to treat the synthetic wastewater from potassium permanganate ions [23].

Despite the great performance and significant efficiency of activated carbon and metallic oxides Nanoparticles, its requirements and conditions of preparation are rather difficult and expensive. Thus, prompted the researchers

Department of Chemistry, Faculty of Science, University of Tabuk, Tabuk 71491, Saudi Arabia. email: s_bantatta@ut.edu.sa

to use low-cost materials within their areas and applied them as adsorbents for permanganate ions adsorption. For instance, sage[24] Neem[25], Nitraria retusa[26], and Ocimum basilicum[27] were used as low-cost sorbents to remove Permanganate anions from synthetic samples.

Foeniculum vulgare plant is well-known by fennel in many countries as shamr in Saudi Arabia, mainly used as food and tea flavored and considered as a flavored spice, its seeds were used as antitumor[28], antimicrobial[29], and antioxidant[30]. Experiments on animals and clinical trials recommend that chronic use of *F. vulgare* plant is not harmful and no toxicity marks were detected [31].

Gold nanoparticles based on seeds extract of fennel *F. vulgare* plant was synthesized and its catalytic activity against rhodamine B and methylene blue days were examined[32], V_2O_5–Fe_2O_3 nanocomposites from stem powder of *F. vulgare* have been also produced and the catalytic performance of nanocomposites particles was assessed for reduction of 4-nitrophenol[33].

Up to now, no adsorbent based on *F. vulgare* seeds was prepared in any form and applied to eliminate the hazardous dyes from water even permanganate ions, despite the excellent medical properties of this herb, in addition to its widespread over the world *F. vulgare* seeds are considered a low-cost material. Therefore, this research mainly aimed to prepare a new adsorbent from seeds of *F. vulgare* and to investigate the adsorbent performance toward eliminating $KMnO_4$ from polluted water. Thermodynamics, Kinetics, and isotherms parameters will also be studied. The performance of this adsorption will be also studied through conditions and impacts that could affect on $KMnO_4$ removal experiment, as the adsorption capacity of modified adsorbent for removal of $KMnO_4$ will be critically addressed.

To achieve all the desired goals of this work and get the best results, unmodified samples from *F. vulgare* seeds have been synthesized and the modification has been also carried out by zinc chloride, copper sulfide, and oxalic acid; both types of samples have been characterized and examined as adsorbents for $KMnO_4$ removal from water, to choose the best adsorbent, the adsorption performances have been compared, then all the $KMnO_4$ adsorption experimental factors and conditions of selected adsorbent were tested.

Materials and methods

Materials. *Foeniculum vulgare* seeds were obtained from a local market in Tabuk City, KSA. All chemicals that were used in this work were obtained from Sigma-Aldrich with a purity of (37%) for hydrochloric acid, ≥ 97% for sodium hydroxide ≥ 97% for zinc chloride, ≥ 99.99% for oxalic acid, ≥ 99:99% for copper sulfide, and ≥ 99.00% for sodium carbonate.

Preparation and modification of adsorbents. The *F. vulgare* seeds were washed with distilled water several times and then dried overnight, after that, the *F. vulgare* seeds powder (FVESP) was obtained by an electric grinder. A sample of 100 g was refluxed for 180 min with 1 L of oxalic acid (20% w/w), afterwards, the mixture was allowed to cool at room temperature. The sold part was separated by filtration, to get rid of any excess amount of oxalic acid; the solid was heated for 90 min with 250 mL of 2 M hydrochloric acid. Then, the filtration of the new mixture was done many times and rinsed with distilled water to have a clean solid, to get rid of any water present in the sample; the solid was left in the oven for 30 h at 130 °C. Finally, to ensure the homogeneity of the sample, the dry solid was grinded and sieved, and the resulted adsorbent of oxalic acid *F. vulgare* seeds powder labeled as (Ox-FVESP).

The same procedure was repeated with mixtures containing 100 g of FVESP with 1 L of 20% w/w acidic solution of zinc chloride, and 100 g FVESP with a mixture of 20% w/w acidic solution of zinc chloride and 50 g of copper sulfide. The resulted adsorbents of zinc chloride *F. vulgare* seeds powder labeled as (Zn-FVESP), and zinc chloride/copper sulfide *F. vulgare* seeds powder (Zn/Cu-FVESP).

Characterization of FVESP adsorbents. To recognize the surface morphology of the modified and unmodified FVESP adsorbents SEM instrument was used at a 10 kV accelerating voltage. And to determine the surface adsorbents' functional groups, the FT-IR instrument (Nicolet iS5 of Thermo Scientific FT-IR, USA) was carried out. The surface area and porosity of each adsorbent were estimated using BET (NOVA-2200 Ver. 6.11) technology for 22 h and 77.35 K. In addition, 40 mL of 0.05 M Na_2CO_3 solutions varying with 2, 4, 6, 8, and 10 initial values of pH_i have been mixed in a 150 mL plastic container with 0.2 g of the idealistic adsorbent. After shaking all containers for 26 h 175 rpm and 27 °C conditions in a shaker incubator, filtration of each was done, then using a pH meter, the final pH (pH_f) of each solution was determined. Finally, to determine the pH_{ZPC} value of this adsorbent, the values of ($pH_i - pH_f$) have been calculated and graphed against the pH_i values.

Adsorption experiments. *The idealistic adsorbent identification.* To determine the superlative as well as the most efficient adsorbent developed in the current study for $KMnO_4$ removal from synthetic aqueous samples, 20 mL of 100 mg L^{-1} $KMnO_4$ solution concentration was combined with 0.03 g of FVESP in a 30 mL amber bottle. A shaker incubator was used for 30 h to stir the sealed amber bottle at 27 °C and 180 rpm. After that, the mixture was filtered; The Jenway UV-6800 UV–Vis spectrophotometer was used at 525 nm to measure the balanced concentration of $KMnO_4$ in the filtrate. The same procedure was repeated with Ox-FVESP, Zn-FVESP, and Zn/Cu-FVESP adsorbents for the $KMnO_4$ adsorption. Equations (1) and (2) were used to calculate the $KMnO_4$ percentage removal percent %R and the quantities of $KMnO_4$ adsorbed at equilibrium Q_e mg g^{-1} by both modified and unmodified adsorbents.

$$\%R = \frac{C - C}{C} 100\% \quad (1)$$

$$Q_e = \frac{V}{m}(C_\circ - C_e) \tag{2}$$

where C° is the $KMnO_4$ initial concentration and C_e is the $KMnO_4$ final concentration, m, and V are the mass of adsorbent (g), and $KMnO_4$ solution volume (L), respectively.

Experimental conditions impact. Batch experiments have been conducted to observe and identify the most significant factors that affect $KMnO_4$ adsorption experiments by ideal adsorbent Ox-FVESP, such as concentration of $KMnO_4$ (10–1400 mg L^{-1}), contact time (0–320 min), the dosage of Ox-FVESP adsorbent (0.005–0.035 g), the adsorption temperature (27–57 °C), and the pH (1.5–11.5). All of the Batch experiments have been done in 30 mL amber bottles by adding 20 mL of $KMnO_4$ solution to enough amounts from Ox-FVESP. A shaker incubator at 180 rpm was used to shake all sealed amber bottles for a required time, followed by filtration of each mixture, and the remaining concentrations of $KMnO_4$ were measured as mentioned previously.

To compute the adsorbed amount of $KMnO_4$ at equilibrium (Q_e, mg g^{-1}) by the Ox-FVESP adsorbent and time t (Q_t, mg g^{-1}) Eqs. (2) and (3) were applied.

$$Q_t = \frac{V}{m}(C_\circ - C_t) \tag{3}$$

where C_t (mg L^{-1}) is the $KMnO_4$ concentration of at contact time.

Temperature impact and isotherm studies. The outcomes obtained from the Batch experiments for 10–1400 mg L^{-1} $KMnO_4$ solutions by 0.02 g by Ox-FVESP adsorbent at 26 h contact time and three different temperatures (27, 42, and 57 °C) and 190 rpm have been analyzed according to the three isotherm models, Langmuir, Freundlich, and Temkin linear forms, Eqs. (4–6) respectively. The parameter of equilibrium R_L value of the Langmuir isotherm model was also evaluated according to Eq. (7).

$$\frac{C_e}{q_e} = \frac{1}{q_{\max} K_L} + \frac{C_e}{q_{\max}} \tag{4}$$

$$\ln q_e = \ln K_F + \frac{1}{n} \ln C_e \tag{5}$$

$$q_e = B_1 \ln K_T + B_1 \ln C_e \tag{6}$$

$$R_L = \frac{1}{1 + K_L C_0} \tag{7}$$

where C_o is the maximum initial concentration of $KMnO_4$ and K_L is the constant of Langmuir, K_F is the constant of Freundlich, and K_T is the constant Temkin. q_{max} (mg g^{-1}) is the maximum capacity of adsorption. B1 and n are constants of the adsorption heat and the intensity of adsorption, respectively.

Contact time impact and Kinetic studies. The experimental data obtained from the adsorption Batch experiments, adsorption of $KMnO_4$ by Ox-FVESP with a concentration of 50, 100, and 200 mg L^{-1} at several times from 0 to 320 min and 27 °C and 190 rpm have been analyzed by three of different kinetic models. Equations (8)–(10), Pseudo 1st order, Pseudo 2nd order, and Intraparticle diffusion, correspondingly. Then, the achieved results have been used to study each of the conducted time impact, rate, and mechanism of $KMnO_4$ adsorption by Ox-FVESP adsorbent.

$$\log(Q_e - Q_t) = \log Q_e - K_1 \frac{t}{2.303} \tag{8}$$

$$\frac{t}{Q_t} = \frac{1}{K_2 Q_e^2} + \frac{t}{Q_e} \tag{9}$$

$$Q_t = K_{dif} \sqrt{t} + C \tag{10}$$

Q_t (mg g^{-1}): the amount of adsorbed $KMnO_4$ at time t, Q_e: the amount of adsorbed $KMnO_4$ at equilibrium, K_1 (1 min^{-1}): rate constants of Pseudo 1st order, K_2: (g mg^{-1} min^{-1}) rate constants of the 2nd order. K_{dif} (mg g^{-1} $min^{-1})^{1/2}$ and C are rate constants of intraparticle diffusion.

Thermodynamic experiment. Constants of thermodynamic ΔG°, ΔH°, and ΔS° have been also evaluated from the outcomes of experimental Conditions impact part for adsorption of 500, 700, 1000, and 1200 mg L^{-1} $KMnO_4$ solutions according to Eqs. (11) and (12).

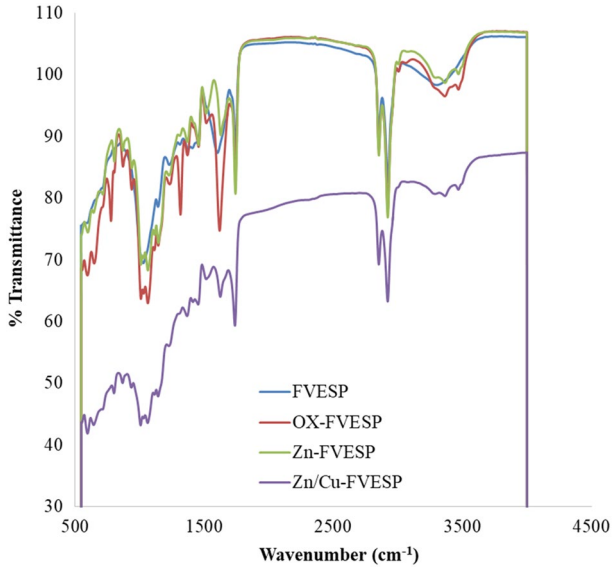

Figure 1. FT-IR for the FVESP and Ox-FVESP and Zn-FVESP and Zn/Cu-FVESP.

$$Ln\left(\frac{Q_e}{Ce}\right) = -\frac{\Delta H^{\circ}}{RT} + \frac{\Delta S^{\circ}}{R} \tag{11}$$

$$\Delta G^{\circ} = \Delta H^{\circ} - T\Delta S^{\circ} \tag{12}$$

where ΔS°, ΔG°, and ΔH° are the change in standard entropy, change in standard free energy, and is the change in standard enthalpy, T and R are the adsorption temperature of (K) and universal gases constant (8.314 J K^{-1} mol), respectively.

Results and discussion

FVESP characterization. The FT-IR spectra of four samples of modified and unmodified FVESP are revealed in Fig. 1. It can be observed from the figure that the unmodified FVESP sample has six peaks at 1060 cm^{-1} for C–O stretching, 1118 cm^{-1} for C–O stretching of a secondary alcohol, 1025 cm^{-1} for C–F stretch Aliphatic fluoro compounds, 1590 cm^{-1} for C=C stretching, 2870 cm^{-1} and 2940 cm^{-1} for stretching the C–H alkane, and 3360 cm^{-1} for hydrogen bond stretching of the O–H. Figure 1 illustrates also that the modified Zn-FVESP, and Zn/Cu-FVESP adsorbents showed the same peaks with a slight shift, while in the case of Ox-FVESP sample, many peaks developed (Fig. 1), and these bands are 1190 cm^{-1}, 1320 cm^{-1}, and 1620 cm^{-1}, The appearance of these bands support the success of the chemical modification process that was carried out for the adsorbent and also confirms the variety of functional groups on the surface of Ox-FVESP, which will have an effective role in permanganate adsorption from the water later.

The spectrum of FVESP, Zn-FVESP, Ox-FVESP, and Zn/Cu-FVESP SEM images are demonstrated in Fig. 2a–d, respectively. When comparing the SEM images of modified samples (b), (c), and (d) to the unmodified adsorbent (a), it can be seen that the surface of the FVESP adsorbent has been significantly transformed by modification procedure, as most of the modified adsorbents pleats have been distorted and their structures became scattered. Furthermore, several heterogeneous holes and pores have appeared on the modified adsorbents surfaces, which improve the adsorption performance. It is also recognized from Fig. 2c that the density of micropores of the modified adsorbent is more than the rest of the other samples.

The relationship between pHi and pHi–pHf is depicted in Fig. 3, which shows that pH_{ZPC} (the solution pH when the surface of sorbent has a zero net charge) is 7.2. Meanwhile, the surface charge of the adsorbent will be positive and negative at solution pH levels lower and higher than 7.2, Al-Aoh[25] has previously found similar findings.

BET surface analyzer results for the modified and unmodified FVESP samples are listed in Table 1, Surface Area (m^2 g^{-1}), Volume of Pore (cm^3 g^{-1}), and Size of Pore (Å). The table shows that the Ox-FVESP sample achieved the highest surface area (0.6806 m^2 g^{-1}) and size of the pore (522.063 Å) compared to the rest of the other samples, The highest values of the surface area and size of pore will positively affect the process of permanganate adsorption on the modified FVESP surface by oxalic acid and prove that the modification process has an important and obvious role.

The idealistic adsorbent identification. Figure 4 illustrates the percentage removal for $KMnO_4$ adsorption by four different samples that were synthesized and modified in this work, and it was as the following 80.52 for FVESP, 64.03 for Zn-FVESP, 89.36 for Ox-FVESP, and 49.08 for Zn/Cu-FVESP. The percentage removal

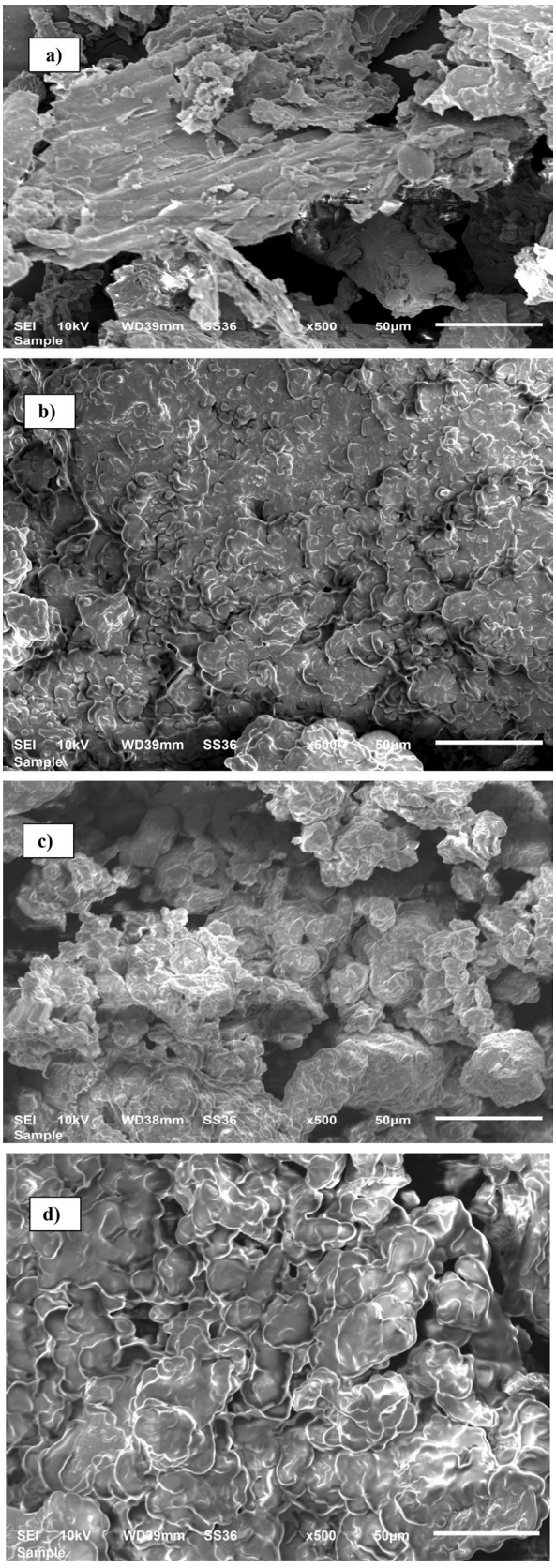

Figure 2. SEM images of (**a**) FVESP and (**b**) Zn-FVESP and (**c**) Ox-FVESP and (**d**) Zn/Cu-FVESP.

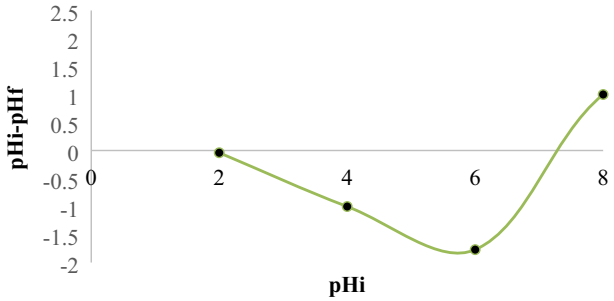

Figure 3. pH_{ZPC} of the Ox-FVESP adsorbent.

Sample	Surface area ($m^2\ g^{-1}$)	Volume of pore ($cm^3\ g^{-1}$)	Size of pore (Å)
FVESP	0.0249	0.00153	53.001
Ox-FVESP	0.6806	0.00215	522.063
Zn-FVESP	0.3087	0.00214	91.717
Zn/Cu-FVESP	0.3979	0.00061	91.037

Table 1. BET surface analyzer of FVESP, Ox-FVESP, Zn-FVESP, and Zn/Cu-FVESP.

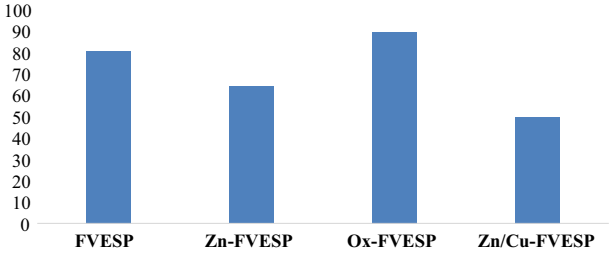

Figure 4. The percentage removal for $KMnO_4$ adsorption by four different samples.

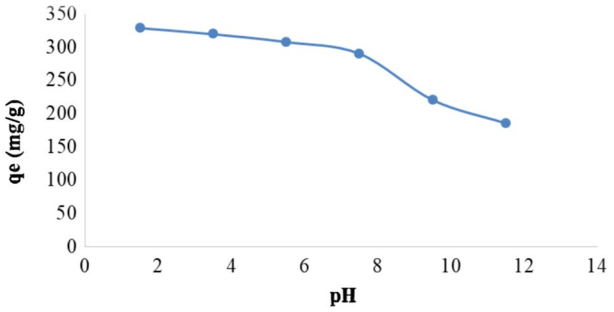

Figure 5. The pH solution impact on the of $KMnO_4$ adsorption by Ox-FVESP adsorbent.

values show that the Ox-FVESP adsorbent has the greatest percentage among other samples, so, these findings support the Ox-FVESP adsorbent is the best sample for $KMnO_4$ adsorption. Also, these results were fully consistent with the SEM and BET surface outcomes. As a result, only Ox-FVESP adsorbent was used in the rest of this study.

Experimental conditions impact. *Influence of pH solution.* The adsorption performance is greatly influenced by the pH of the adsorbate solution, degree of ionization, and charge of adsorbent of the dye molecules also impacted by pH. As a result, the impact of this issue was addressed in this study (Fig. 5). It is clear from the figure that the *qe* (mg g^{-1}) value was greatly affected by the pH values, as it was high when pH values were raised from 1.5 to 7.2, and this is due to the high attraction between the positive charges of the Ox-FVESP surface and

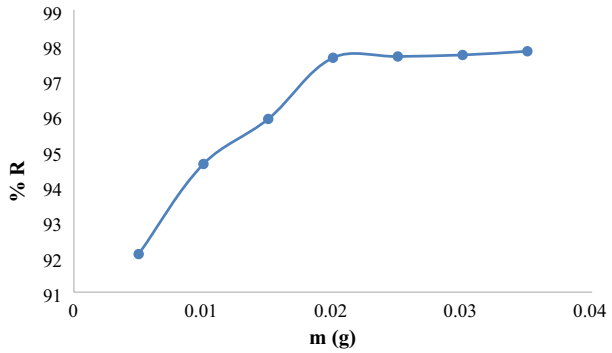

Figure 6. Effect of dose on adsorption performance of Ox-FVESP for $KMnO_4$.

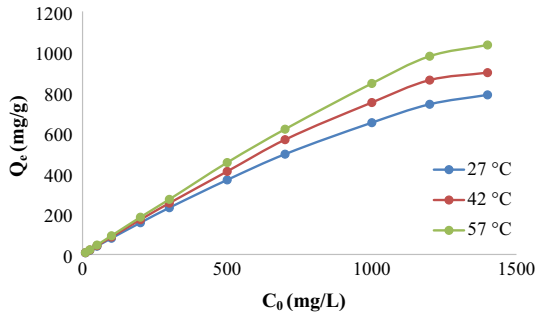

Figure 7. Impacts of initial concentration and temperature on the $KMnO_4$ adsorption by Ox-FVESP.

the MnO_4^- anions. In contrast, increasing the pH value over 7.2 has a negative effect on *qe* (mg g^{-1}) because of the significant repulsion between the negative MnO_4^- ions and the negative charges of this adsorbent surface. Like results have been found for the $KMnO_4$ elimination by chemically modified sage leaves powder[24].

Impact of Ox-FVESP doses. To specify the ideal mass of Ox-FVESP that will be required for the $KMnO_4$ adsorption the percent removal of $KMnO_4$ was plotted against Ox-FVESP doses (Fig. 6). The values of percent removal of $KMnO_4$% R are improved by increasing the mass of Ox-FVESP from 0.005 to 0.020 g. This rise was caused by the improvement of the active sites on the Ox-FVESP surface, which is related to the adsorbent quantity[34]. Figure 6 shows also the percent R value does not change significantly when the mass of the adsorbent is increased from 0.020 to 0.035 g and it is assumed that the amount of dye adsorption was significantly affected by the concentration of unfilled dynamic reactive sites due to the bonding ability of the adsorption surface function[35,36]. In this study, 0.020 g of Ox-FVESP was chosen as the optimal dose. The adsorption of CR dye by Zn/Cu-TPLLP adsorbent[23] and $KMnO_4$ on the CuS surface showed a similar Patten[37].

Temperature impact and isotherm studies. The impact of initial solution concentration and temperature on the adsorption capacity of this work is demonstrated in Fig. 7. Figure 7 shows the relationship between the adsorption amount Q_e (mg/g) and the concentration of $KMnO_4$ (10–1400 mg L^{-1}) at 27, 42, and 57 °C temperatures. It can be observed from the figure that raising the temperature of the solution has a positive impact on the adsorption capacity of $KMnO_4$ by Ox-FVESP. And this refers to the decreasing of $KMnO_4$ viscosity with solution temperature increasing, also, the kinetic energy of the permanganate particles increases with rising the temperature; the same kinetic energy performance for permanganate ions was recorded by neem leaves powder adsorbent[25]. It is also noted from the same figure that the adsorption of permanganate is improved by raising the concentration of $KMnO_4$ from 10 to 1400 (mg L^{-1}) at the same temperature. And this could be supported by the finding that raising the adsorbate concentration will develop the dynamic force[38], which lowers the resistance of $KMnO_4$ particles mass movement between the Ox-FVESP surface and adsorbate solution. It is also clear that the adsorbent will be effective even at $KMnO_4$ concentrations higher than 1400 mg L^{-1}, and this is refer to the unfilled adsorption sites on the adsorbent surface.

Moreover, The outcomes obtained from Batch experiments were analyzed according to the isotherm model of Langmuir (Ce against Ce/qe), isotherm model of Freundlich (ln Ce against ln qe), and isotherm model of Temkin (ln Ce against qe) Fig. 8a–c, the slopes and intercepts of these plots were used to achieve the isotherm parameters and presented in Table 2. Where the experimental results are well fitted by applying the Langmuir isotherm model and the R^2 values were the highest compared with Freundlich and Temkin models Table 2, which approves that the Langmuir model is the best fit for this adsorption. These findings also show that the adsorption of $KMnO_4$ is monolayer adsorption and that the Ox-FVESP adsorption sites are homogeneous. Same outputs for

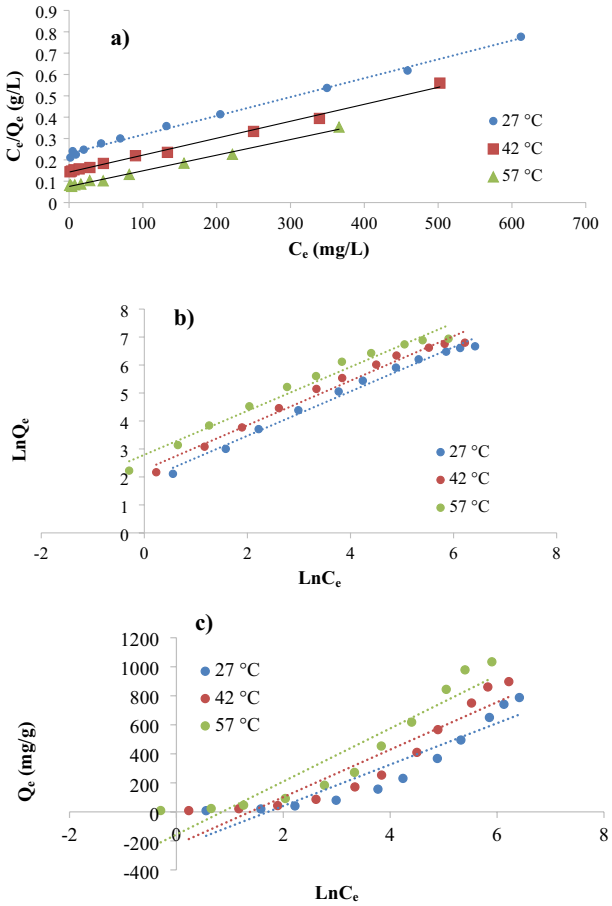

Figure 8. (**a**) Langmuir and (**b**) Freundlich and (**c**) Temkin isotherm models for adsorption of $KMnO_4$ by Ox-FVESP.

Temperature	Isotherm parameters										
	Langmuir				Freundlich				Temkin		
	q_{max} (mg g^{-1})	K_L (L mg^{-1})	R_L	R^2	K_F (mg g^{-1}) (L $mg^{-1})^{1/n}$	1/n	n	R^2	K_T (L mg^{-1})	B_1	R^2
27 °C	1111.11	0.00392	0.15408	0.996	6.2557	0.792	1.2625	0.988	0.18027	142.58	0.871
42 °C	1250.00	0.00561	0.11294	0.994	9.5735	0.796	1.2560	0.982	0.25209	163.59	0.878
57 °C	1428.57	0.00928	0.07144	0.994	13.6154	0.785	1.2740	0.975	0.42520	182.81	0.886

Table 2. Isotherm constants of Langmuir and Freundlich and Temkin models for $KMnO_4$ adsorption by Ox-FVESP.

$KMnO_4$ adsorption as recorded by a chemical modified powder from leaves of neem[25]. Moreover, the Favorable adsorption was confirmed by values of R_L which ranged between 0 and 1[14].

Furthermore, high adsorption capacities of 1111.11, 1250.00, and 1428.57 mg g^{-1} (Table 2) were achieved, at three temperatures that were used in this study. This demonstrates that Ox-FVESP, as a low-cost and very effective adsorbent, will be of particular importance in the purification of wastewaters from the $KMnO_4$.

Contact time impact and Kinetic studies. To investigate the contact time impact on the $KMnO_4$ adsorption experiment, the contact time (t) has been graphed against Q_t (mg g^{-1}) (adsorption quantity at such time t) for the adsorption of (50, 100, and 200 mg L^{-1}) $KMnO_4$ concentrations by the ideal dose of chemically modified FVESP adsorbent selected for this work (Fig. 9). Figure 9 shows that there are three adsorption regions, the higher adsorption was detected at region I (0–16 min) where the adsorption amount (Q_t) rapidly augmented, while the increase in region II (16–64 min) was regularly and after 64 min till the end of the experiment time, it was practically consistent (region III). Initially, the removal rate was high due to the availability of the abundant of functional groups[39]. Similarly, the sharp increase in the rate of removal at the beginning of the adsorption process showed the strong attraction forces between OX-FVESP sites and $KMnO_4$. The same results for $KMnO_4$

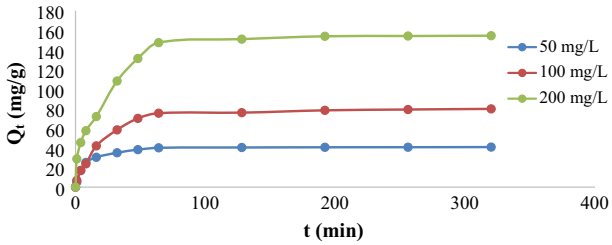

Figure 9. Impact of adsorption time on $KMnO_4$ adsorption by Ox-FVESP.

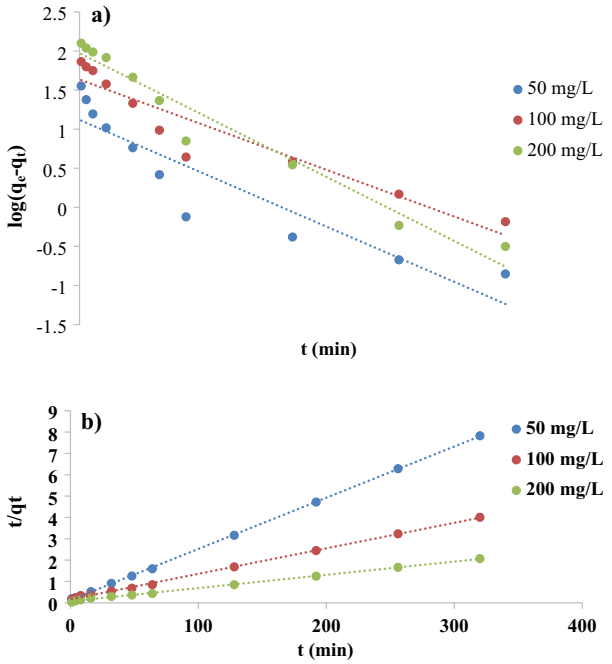

Figure 10. (**a**) Kinetic model of the 1st order and (**b**) Kinetic model of the 2nd order for $KMnO_4$ adsorption by Ox-FVESP.

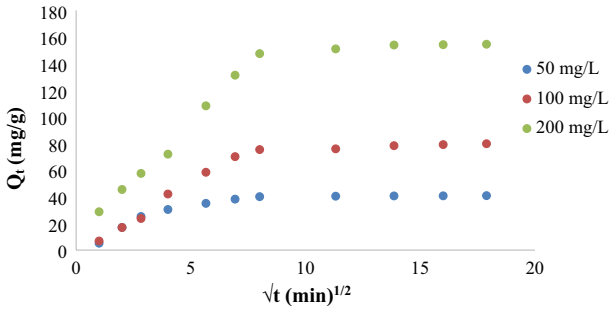

Figure 11. Model of intra-particle diffusion for $KMnO_4$ adsorption by Ox-FVESP.

adsorption were obtained by a powder of sage leaves modified by zinc chloride[24] and for the adsorption of Cu(II) ions on the nanomaterials surface adsorbent[40]. It is also noted from the same figure that the equilibrium time occurred at the 45th minute of the experiment time.

Furthermore, the experimental outcomes of this adsorption have been studied according to Pseudo-first order, pseudo-second order, and Intraparticle diffusion kinetics models Figs. 10a,b, and 11. The slopes and intercepts of these plots were used to calculate the kinetic parameters and summarized in Tables 3 and 4, the linear relationships observed by applying the pseudo-second order model in Fig. 10b, where the highest R^2 values occurred,

C_0 (mg L^{-1})	$Q_{e,exp}$ (mg g^{-1})	Kinetic model						
		1st order			2nd order			
		$Q_{e1,cal}$ (mg g^{-1})	K_1 (h^{-1})	R^2	$Q_{e2,cal}$ (mg g^{-1})	K_2 (g mg^{-1} h^{-1})	R^2	Rate
50	40.89	13.14	0.0212	0.85	41.67	0.0046	0.999	0.19308
100	79.87	43.14	0.0180	0.898	83.33	0.0009	0.999	0.07481
200	154.57	93.86	0.0246	0.958	161.29	0.0005	0.998	0.08832

Table 3. Parameters of the 1st and 2nd-order kinetic models for adsorption of $KMnO_4$ by Ox-FVESP.

C_o (mg L^{-1})	First region			Second region		
	K_{dif} (mg $h^{-1/2}$ g)	C	R^2	K_{dif} (mg $h^{-1/2}$ g)	C	R^2
50	5.187	5.839	0.889	0.0743	39.59	0.973
100	10.990	9.413	0.993	0.4868	71.27	0.945
200	17.271	− 4.389	0.982	0.7332	142.44	0.900

Table 4. Parameters of the intra-particle-diffusion kinetic model for $KMnO_4$ adsorption by Ox-FVESP.

Initial concentration (mg L^{-1})	ΔH° (kJ mol^{-1})	ΔS° (kJ mol^{-1})	ΔG° (KJ mol^{-1})			R^2
			300 K	315 K	330 K	
500	34.371	0.1227	− 2.4260	− 4.2659	− 6.1057	0.977
700	31.346	0.1117	− 2.1758	− 3.8519	− 5.5280	0.999
1000	29.246	0.1024	− 1.4849	− 3.0214	− 4.5580	0.992
1200	27.541	0.0956	− 1.1374	− 2.5713	− 4.0051	0.992

Table 5. Thermodynamic constants for $KMnO_4$ adsorption by Ox-FVESP.

and the good agreement between the experimental Q_e values (Table 3) and computed values of Q_e, which approve that the adsorption of this work followed the second-order kinetic model. And implying that the biosorption of $KMnO_4$ from the aqueous media is governed by a chemical kinetic mechanism involving electron exchange or sharing between the anionic part of the dye (MnO_4^-) and the functional groups on the OX-FVESP adsorbent surface. Similar findings were stated for $KMnO_4$ adsorption by activated carbon[12], nanoparticles prepared from copper sulfide[23], and powder sage leaves modified by zinc chloride[24]. The dye adsorption process by modified activated carbon adsorbents followed also the pseudo-second order[41,42].

Intra-particle diffusion plots for $KMnO_4$ adsorption by Ox-FVESP (Fig. 10) and R^2 values, Table 4 display that the relationship between contact time (t) and adsorption amount (Q_t) could not be linear at all, but two different areas are observed. Furthermore, all the plots do not cross the original and this approves that the adsorption of MnO_4^- ions is not affected by the Intra-particle diffusion step; migration of MnO_4^- ions via the Ox-FVESP pores will be very simple. This agrees with the SEM results, as it was clear that the Ox-FVESP surface has a lot of asymmetrical pores.

Thermodynamic experiment. Equation (11) was applied to evaluate parameters of the thermodynamic ΔH°, and ΔS° at three different temperatures for solution Initial concentrations 500, 700, 1000, and 1200 mg L^{-1}. Then, the values of ΔG° were computed according to Eq. (12) based on the previously calculated values of ΔS° and ΔH° and illustrated in Table 5. The lowering in the randomness and the endothermic process of permanganate adsorption by Ox-FVESP adsorbent was confirmed by the positive values of each ΔS° and ΔH° (Table 5)[26]. Moreover, the ΔH° values are higher than 20.9 kJ mol^{-1}, ranging from 27.541 to 34.371 kJ mol^{-1}, which indicates the molecules of adsorbate were chemically adsorbed at the adsorbent surface sites, these results are in agreement with the previous kinetic outputs. Negative values of ΔG° suggest spontaneous adsorption in the range of temperature that is used in this study, similar findings were stated for $KMnO_4$ adsorption by modified Powder of Ocimum basilicum[26] and other adsorbents developed from very low-cost adsorbents[23,24], the adsorption process by cationic polymeric adsorbent also achieved similar results[43].

Comparative study with other adsorbents. Table 6 summarized the adsorption capacities of $KMnO_4$ removal by Ox-FVESP at three temperatures and the capacities of other synthesized low-cost adsorbents. As presented in Table 6, Ox-FVESP adsorbent has a higher adsorption capacity than the conventional low-cost adsorbents that were previously employed to remove $KMnO_4$ from aqueous samples. As a result, the cost-effectiveness of Ox-FVESP, easy availability, and its high performance in adsorption of permanganate from polluted water give this adsorbent a strong opportunity over other adsorbents.

Adsorbant	Temperature (°C)	Q (mg g^{-1})	Reference
Ox-FVESP	27	1111.11	This study
	42	1250.00	
	57	1428.57	
Granular activated charcoal		57.47	[1]
Animal bone-derived activated carbon		28.04	[14]
Corncob derived activated carbon		26.00	[14]
Coconut shells derived activated carbon		23.25	[12]
Modified activated carbonaceous materials		100.00	[15]
Zinc chloride *Ocimum basilicum* leaves powder	25	588.235	[37]
	35	625.000	
	45	666.667	
	55	714.286	

Table 6. Adsorption capacities for $KMnO_4$ removal by several adsorbents.

Conclusions

Modification of the *F. vulgare* Seeds (FVES) powder was done by each of $ZnCl_2$, oxalic acid, and CuS, all samples have been characterized by different techniques and examined for permanganate ($KMnO_4$) adsorption. Among the four modified and unmodified samples, the sample modified by oxalic acid (Ox-FVESP) has the highest percentage removal for $KMnO_4$ adsorption (%R = 89.36), and was nominated as a new adsorbent for $KMnO_4$ adsorption from the synthesized solutions. The surface area, volume, and size of the pore of the Ox-FVESP adsorbent were determined as 0.6806 m^2 g^{-1}, 0.00215 cm^3 g^{-1}, and 522.063 Å, respectively, as pH_{ZPC} also was stated to be 7.2. The influence of $KMnO_4$ concentration, Ox-FVESP dose, pH of the solution, adsorption temperature, and adsorption time on the $KMnO_4$ adsorption was inspected, it can be noted from the experimental outcomes the adsorption performance of $KMnO_4$ was positively affected by the rising concentration of $KMnO_4$ from 10 to 1400 mg L^{-1}, Ox-FVESP dose from 0.005 to 0.020 g, contact temperature from 27 to 57 °C, and adsorption time from 0 to 64 min. While the increase of solution pH from 1.5 to 11.5 has a negative effect on the adsorption process. The calculated R^2 values of different isotherm and kinetic models (0.999 and 0.996) revealed the adsorption performance of $KMnO_4$ following the Langmuir and Pseudo 2nd order models. Constants of thermodynamic ΔG°, ΔH°, and ΔS° values indicate chemical and spontaneous adsorption at the adsorbent surface. Additionally, high adsorption capacities were accomplished at three temperatures that were used in this work 1111.11, 1250.00, and 1428.57 mg g^{-1}. Proposing that the Ox-FVESP adsorbent prepared from very low-cost material was important to explore the use in the water purification from dye at optimum conditions.

Data availability

The datasets used and/or analyzed during the current study are available from the corresponding author on reasonable request. And I state that the experimental research on plant seeds used in this study complied with the relevant institutional, national, and international guidelines and legislation.

Received: 10 January 2022; Accepted: 7 March 2022
Published online: 16 March 2022

References

1. Verma, R. K., Kapoor, R., Gupta, S. K. & Chaudhari, R. R. An efficient technique for removal of K+ and MnO_4– ions through adsorption in aqueous solution by using activated charcoal. *Pharm. Chem. J.* **1**, 20–25 (2014).
2. Elsheikh, M. A. E. S., Guirguis, H. S. & Amer, A. Removal of iron and manganese from groundwater: A study of using potassium permanganate and sedimentation. *Bull. Faculty Eng. Mansoura Univ.* **42**(3), 7–12 (2020).
3. Ahmad, A. *et al.* Arsenite removal in groundwater treatment plants by sequential Permanganate–Ferric treatment. *J. Water Process. Eng.* **26**, 221–229 (2018).
4. Rodríguez, E. *et al.* Oxidative elimination of cyanotoxins: Comparison of ozone, chlorine, chlorine dioxide and permanganate. *Water Res.* **41**(15), 3381–3393 (2007).
5. He, D., Guan, X., Ma, J., Yang, X. & Cui, C. Influence of humic acids of different origins on oxidation of phenol and chlorophenols by permanganate. *J. Hazard. Mater* **182**(1–3), 681–688 (2010).
6. Liu, C. *et al.* Dependence of sulfadiazine oxidative degradation on physicochemical properties of manganese dioxides. *Ind. Eng. Chem. Res.* **48**(23), 10408–10413 (2009).
7. Jiang, J., Pang, S. Y. & Ma, J. Oxidation of triclosan by permanganate (Mn (VII)): Importance of ligands and in situ formed manganese oxides. *Environ. Sci. Technol* **43**(21), 8326–8331 (2009).
8. Kao, C. M., Huang, K. D., Wang, J. Y., Chen, T. Y. & Chien, H. Y. Application of potassium permanganate as an oxidant for in situ oxidation of trichloroethylene-contaminated groundwater: A laboratory and kinetics study. *J. Hazard. Mater* **153**(3), 919–927 (2008).
9. Hazardous Substance Fact Sheet, Potassium Permanganate, New Jersy Department of Health and Senior Services, March 1986, Revised May 2002, p. 2–6. (2002).
10. Abdeen, Z., Mohammad, S. G. & Mahmoud, M. S. Adsorption of Mn (II) ion on polyvinyl alcohol/chitosan dry blending from aqueous solution. *Environ. Nanotechnol. Monit. Manag* **3**, 1–9 (2015).
11. Li, G. X., Huaug, Y. H., Chen, T. C., Shih, Y. J. & Zhang, H. Reduction and immobilization of potassium permanganate on iron oxide catalyst by fluidized-bed crystallization technology. *Appl. Sci* **2**(1), 166–174 (2012).

12. Aprilliani, F., Warsiki, E., & Iskandar, A. Kinetic studies of potassium permanganate adsorption by activated carbon and its ability as ethylene oxidation material. in *IOP Conference Series: Earth and Environmental Science* Vol. 141, No. 1, 012003. (IOP Publishing, 2018).
13. Mahmoodi, N. M., Taghizadeh, M. & Taghizadeh, A. Mesoporous activated carbons of low-cost agricultural bio-wastes with high adsorption capacity: Preparation and artificial neural network modeling of dye removal from single and multicomponent (binary and ternary) systems. *J. Mol. Liq* **269**, 217–228 (2018).
14. Ezeugo, D. J. & Anadebe, C. V. Removal of potassium permanganate from aqueous solution by adsorption onto activated carbon prepared from animal bone and corn cob. *Equatorial J. Eng.* **2018**, 14–21 (2018).
15. Mahmoud, M. E., Yakout, A. A., Saad, S. R. & Osman, M. M. Removal of potassium permanganate from water by modified carbonaceous materials. *Desalination Water Treat* **57**(33), 15559–15569 (2016).
16. Fangwen, L. I., Xiaoai, W. U., Songjiang, M. A., Zhongjian, X. U., Wenhua, L. I. U., & Fen, L. I. U. Adsorption and desorption mechanisms of methylene blue removal with iron-oxide coated porous ceramic filter. *J. Water Resource Prot.* **2009**, 35–40 (2009)
17. Rani, S., Aggarwal, M., Kumar, M., Sharma, S. & Kumar, D. Removal of methylene blue and rhodamine B from water by zirconium oxide/graphene. *Water Sci.* **30**(1), 51–60 (2016).
18. Tavakkoli, H. & Hamedi, F. Synthesis of $Gd_{0.5}Sr_{0.5}FeO_3$ perovskite-type nanopowders for adsorptive removal of MB dye from water. *Res. Chem. Intermed.* **42**(4), 3005–3027 (2016).
19. Chin, L. Y., Pei, L. Y., & Binti Rosli, R. Immobilization of nano-sized TiO_2 on glass plate for the removal of methyl orange and methylene blue. in *ICGSCE 2014*, 105–113. (Springer, 2015).
20. Yang, S. T. *et al.* Removal of methylene blue from aqueous solution by graphene oxide. *J. Colloid Interface Sci.* **359**(1), 24–29 (2011).
21. Mustafa, G., Tahir, H., Sultan, M. & Akhtar, N. Synthesis and characterization of cupric oxide (CuO) nanoparticles and their application for the removal of dyes. *Afr. J. Biotechnol.* **12**(47), 6650–6660 (2013).
22. Al-Aoh, H. A. *et al.* Removal of methylene blue from synthetic wastewater by the selected metallic oxides nanoparticles adsorbent: Equilibrium, kinetic and thermodynamic studies. *Chem. Eng. Commun.* **207**(12), 1719–1735 (2020).
23. Aljohani, M. M. & Al-Aoh, H. A. Adsorptive removal of permanganate anions from synthetic wastewater using copper sulfide nanoparticles. *Mater. Res. Express.* **8**(3), 035012 (2021).
24. Bani-Atta, S. A. Zinc chloride modification of sage leaves powder and its application as an adsorbent for $KMnO_4$ removal from aqueous solutions. *Mater. Res. Express* **7**(9), 095511 (2020).
25. Al-Aoh, H. A. Equilibrium, thermodynamic and kinetic study for potassium permanganate adsorption by Neem leaves powder. *Desalination Water Treat* **170**, 101–110 (2019).
26. Al-Aoh, H. A. Adsorption of MnO4– from aqueous solution by Nitraria retusa leaves powder; kinetic, equilibrium and thermodynamic studies. *Mater. Res. Express.* **6**(11), 115102 (2019).
27. Alamrani, N. A., Al-Aoh, H. A., Aljohani, M. M., Bani-Atta, S. A., Sobhi, M., Syed Khalid, M., et al. Wastewater purification from permanganate ions by sorption on the *Ocimum basilicum* leaves powder modified by zinc chloride. *J. Chem.* **2021**, 1–10 (2021).
28. Badgujar, S. B., Patel, V. V., & Bandivdekar, A. H. *Foeniculum vulgare* Mill: A review of its botany, phytochemistry, pharmacology, contemporary application, and toxicology. *Biomed. Res. Int.* **2014**, 1–32 (2014).
29. Purkayastha, S., Narain, R. & Dahiya, P. Evaluation of antimicrobial and phytochemical screening of Fennel, Juniper and Kalonji essential oils against multi drug resistant clinical isolates. *Asian Pac. J. Trop. Biomed.* **2**(3), S1625–S1629 (2012).
30. Roby, M. H. H., Sarhan, M. A., Selim, K. A. H. & Khalel, K. I. Antioxidant and antimicrobial activities of essential oil and extracts of fennel (*Foeniculum vulgare* L.) and chamomile (*Matricaria chamomilla* L.). *Ind. Crops Prod.* **44**, 437–445 (2013).
31. Shah, A. H., Qureshi, S. & Ageel, A. M. Toxicity studies in mice of ethanol extracts of *Foeniculum vulgare* fruit and *Ruta chalepensis* aerial parts. *J. Ethnopharmacol.* **34**, 167–172 (1991).
32. Choudhary, M. K., Kataria, J. & Sharma, S. A biomimetic synthesis of stable gold nanoparticles derived from aqueous extract of *Foeniculum vulgare* seeds and evaluation of their catalytic activity. *Appl. Nanosci* **7**(7), 439–447 (2017).
33. Yulizar, Y., Apriandanu, D. O. B. & Al Jabbar, J. L. Facile one-pot preparation of V2O5-Fe2O3 nanocomposites using *Foeniculum vulgare* extracts and their catalytic property. *Inorg. Chem. Commun.* **123**, 108320 (2021).
34. Kuchekar, S. R., Patil, M. P., Gaikwad, V. B. & Han, S. H. Synthesis and characterization of silver nanoparticles using *Azadirachta indica* (Neem) leaf extract. *IJESI* **6**(4), 47–55 (2017).
35. Nekouei, F., Nekouei, S., Tyagi, I. & Gupta, V. K. Kinetic, thermodynamic and isotherm studies for acid blue 129 removal from liquids using copper oxide nanoparticle-modified activated carbon as a novel adsorbent. *J. Mol. Liq.* **201**, 124–133 (2015).
36. Hasan, M. M. *et al.* Natural biodegradable polymeric bioadsorbents for efficient cationic dye encapsulation from wastewater. *J. Mol. Liq.* **323**, 114587 (2021).
37. Alamrani, N. A., & Al-Aoh, H. A. Elimination of congo red dye from industrial wastewater using *Teucrium polium* L. as a low-cost local adsorbent. *Adsorp. Sci. Technol.* **2021**, 1–12 (2021).
38. Baocheng, Q. U. *et al.* Adsorption behavior of Azo Dye CI Acid Red 14 in aqueous solution on surface soils. *J. Environ. Sci.* **20**(6), 704–709 (2008).
39. Awual, M. R. A facile composite material for enhanced cadmium (II) ion capturing from wastewater. *J. Environ. Chem. Eng.* **7**(5), 103378 (2019).
40. Awual, M. R. New type mesoporous conjugate material for selective optical copper (II) ions monitoring & removal from polluted waters. *Chem. Eng. J* **307**, 85–94 (2017).
41. Mahmoodi, N. M., Taghizadeh, M. & Taghizadeh, A. Activated carbon/metal-organic framework composite as a bio-based novel green adsorbent: Preparation and mathematical pollutant removal modeling. *J. Mol. Liq* **277**, 310–322 (2019).
42. Hayati, B. & Mahmoodi, N. M. Modification of activated carbon by the alkaline treatment to remove the dyes from wastewater: Mechanism, isotherm and kinetic. *Desalination Water Treat* **47**(1–3), 322–333 (2012).
43. Mahmoodi, N. M., Sadeghi, U., Maleki, A., Hayati, B. & Najafi, F. Synthesis of cationic polymeric adsorbent and dye removal isotherm, kinetic and thermodynamic. *JIEC* **20**(5), 2745–2753 (2014).

Acknowledgements

The authors are appreciative to the University of Tabuk's Faculty of Science for their assistance and facilities in completing this work.

Author contributions

Methodology, validation, conceptualization formal analysis, investigation, writing—original draft, writing—reviewing & editing.

Competing interests

The author declares no competing interests.

Additional information

Correspondence and requests for materials should be addressed to S.A.B.-A.

Reprints and permissions information is available at www.nature.com/reprints.

Publisher's note Springer Nature remains neutral with regard to jurisdictional claims in published maps and institutional affiliations.